Title

The Scanner as the Stimulus: Deficient Gamma-BOLD Coupling in Schizophrenia at Rest.

Journal

Schizophrenia Bulletin: The Journal of Psychoses and Related Disorders, 49(5)

Authors

Jacob, Michael
Sargent, Kaia
Roach, Brian
et al.

Publication Date

2023-09-07

DOI

10.1093/schbul/sbad014

Peer reviewed

Schizophrenia Bulletin vol. 49 no. 5 pp. 1364–1374, 2023
https://doi.org/10.1093/schbul/sbad014
Advance Access publication April 25, 2023

The Scanner as the Stimulus: Deficient Gamma-BOLD Coupling in Schizophrenia at Rest

Michael S. Jacob[*,1,2,3], Kaia Sargent[1,3], Brian J. Roach[1], Elhum A. Shamshiri[1], Daniel H. Mathalon[1,2], and Judith M. Ford[1,2]

[1]Mental Health Service, San Francisco VA Medical Center, 4150 Clement St, San Francisco, CA 94121, USA; [2]Department of Psychiatry and Weill Institute for Neurosciences, University of California, San Francisco, San Francisco, CA, USA

[3]These authors contributed equally to this work.

*To whom correspondence should be addressed; Mental Health Service, San Francisco Veterans Affairs Healthcare System, 4150 Clement Street, San Francisco, CA 94121, USA; tel: 415-221-4810 ext. 23972, fax: 415-750-6622, e-mail: Michael.Jacob@ucsf.edu

Functional magnetic resonance imaging (fMRI) scanners are unavoidably loud and uncomfortable experimental tools that are necessary for schizophrenia (SZ) neuroscience research. The validity of fMRI paradigms might be undermined by well-known sensory processing abnormalities in SZ that could exert distinct effects on neural activity in the presence of scanner background sound. Given the ubiquity of resting-state fMRI (rs-fMRI) paradigms in SZ research, elucidating the relationship between neural, hemodynamic, and sensory processing deficits during scanning is necessary to refine the construct validity of the MR neuroimaging environment. We recorded simultaneous electroencephalography (EEG)-fMRI at rest in people with SZ (n = 57) and healthy control participants without a psychiatric diagnosis (n = 46) and identified gamma EEG activity in the same frequency range as the background sounds emitted from our scanner during a resting-state sequence. In participants with SZ, gamma coupling to the hemodynamic signal was reduced in bilateral auditory regions of the superior temporal gyri. Impaired gamma-hemodynamic coupling was associated with sensory gating deficits and worse symptom severity. Fundamental sensory-neural processing deficits in SZ are present at rest when considering scanner background sound as a "stimulus." This finding may impact the interpretation of rs-fMRI activity in studies of people with SZ. Future neuroimaging research in SZ might consider background sound as a confounding variable, potentially related to fluctuations in neural excitability and arousal.

Key words: schizophrenia/resting-state/EEG-fMRI/gamma/excitation-inhibition balance/sensory gating

Introduction

Signal processing aberrancy in schizophrenia (SZ) spans sensory,[1] motor,[2] and cognitive domains.[3] Rather than reflecting a singular neuroanatomical deficit or specific network dysfunction, these composite abnormalities point toward global brain dysfunction,[4] potentially arising from a fundamental excitatory-inhibitory (E/I) imbalance.[5–8] Relating cellular abnormalities to human neurophysiology in patients with SZ remains a central translational challenge that depends on the construct validity of neuroimaging paradigms: does functional magnetic resonance imaging (fMRI) measure what we think it measures? Is resting-state really at "rest"?

Electroencephalography (EEG) can be used to identify putative biomarkers of E/I balance. There has been recent interest in the physiological significance of periodic (oscillatory) and aperiodic (broadband or non-oscillatory) components of the EEG signal,[9] which may offer complementary indices of E/I balance. Gamma oscillations are generated through coordinated interactions between excitatory and inhibitory currents,[10,11] principally mediated by inhibitory interneurons,[8] and that may be impaired in SZ.[12] Alterations in gamma power in SZ are therefore thought to relate to disturbances in inhibitory transmission and E/I balance.[13–16] In event-related EEG studies of SZ patients, gamma abnormalities are linked to stimulus-specific processing deficits, most notable in auditory paradigms[17–22] that are linked to impaired sensory gating[23] and auditory hallucinations.[24]

E/I balance may also be inferred from the slope of the local field potential or EEG power spectrum reflecting aperiodic activity.[25–27] This can be accomplished by estimating the slope of a linear fit to EEG spectra after

log-log transformation of frequency and power. The aperiodic exponent is estimated by β, in the $1/f^{\beta}$ model, and is equivalent to the negative slope in log-log space. Gao et al.[27] have shown that increasing synaptic inhibition, through computational models, and experimentally through the administration of a GABAergic anesthetic, results in a significant increase (steepening) of the aperiodic slope. In contrast with gamma rhythms, which tend to reflect local processing dynamics, the aperiodic slope may capture global brain states such as the level of consciousness, sleep, and arousal.[28–31]

Defining the relationship between E/I biomarkers and regional changes in ongoing hemodynamic activity is necessary to bridge cellular neuroscience, human electrophysiology, and resting-state fMRI (rs-fMRI) studies in SZ. However, EEG biomarkers might be sensitive to experimental factors, such as scanner sound, that impinge on "pure" resting-state conditions. That is, neural activity may be driven by background stimuli that are unavoidable, such as scanner background sound,[32] and that may also drive arousal.[33] In healthy control (HC) participants, we have previously observed that gamma power fluctuations were associated with BOLD activity in locally circumscribed auditory regions, whereas aperiodic power fluctuations were associated with distributed networks, including auditory, cerebellar, salience, and prefrontal regions.[34] We previously hypothesized that EEG measures of E/I balance might reflect processing of scanner background sound and spontaneous fluctuations in arousal during the resting-state.

In this current study, we hypothesized that E/I imbalance in SZ might be revealed from reduced gamma power (deficient local inhibitory current) and flatter aperiodic slope (globally deficient inhibition) and associated with atypical regional and distributed BOLD signals. We further hypothesized that aberrant gamma and aperiodic activity would reflect ongoing processing of scanner background sound and would be associated with subjective impairment in the gating of environmental auditory stimuli.

Using simultaneous EEG-fMRI, we first measure aperiodic and gamma EEG signals in HC and SZ participants while at rest and then use those signals as predictors in a whole-brain, parametric modulation analysis to test for group differences in EEG-BOLD coupling. Contrary to our initial hypothesis, we find no group differences in resting-state gamma or aperiodic EEG. However, we do find reduced BOLD coupling to gamma EEG in regions of the auditory cortex in SZ that are associated with impaired sensory gating. Our results have implications for rs-fMRI paradigms and studies of SZ in particular: changes in resting-state activity may be driven by unavoidable scanner background stimuli.

Methods

Participants

The study included 57 people with SZ (n = 45) and schizoaffective disorder (n = 12, collectively referred to as SZ), and 46 HC participants matched for age and gender. One SZ and two HC participants had no usable EEG data collected during fMRI recording due to an amplifier connection problem and were excluded from the analysis. Participants were recruited through advertising and word of mouth, and SZ participants were referred by community outpatient clinics. Clinical and demographic data are presented in table 1. The HC participant sample and analysis have been previously reported.[38]

For both groups, exclusion criteria included substance abuse in the past 3 months, any significant medical or neurological illness, or head injury resulting in loss of consciousness. In addition, HC was excluded for any current or past psychiatric disorder based on the Structured Clinical Interview for DSM-IV (SCID-IV), any history

Table 1. Group Demographic Data

	Schizophrenia Mean (SD) [Range]	Healthy Control Mean (SD) [Range]	Between-group Comparison *P*-value
Number of participants	57	46	
Age (years)	35.6 (13.9) [18–62]	38.3 (15.1) [18–69]	.339
Gender	11F, 46M	9F, 37M	.985
Average parental SES[a]	36.3 (18.1)	34.6 (18.6)	.535
Handedness[b]	52R, 2L, 3A	41R, 2L, 3A	.95
Estimated IQ[c]	108.9 (8.85)	111.3	.217
Antipsychotic medication	13U, 39A, 4T, 1A + T	46U	
PANSS total	65.43 (34.06)		
PANSS positive total	16.84 (6.69)		
PANSS negative total	17.16 (5.86)		
SGI total	63.82 (34.06)		

Note: PANSS, Positive and Negative Syndrome Scale; SGI, Sensory Gating Inventory
[a]The Hollingshead four-factor index.[35] Lower scores represent higher socioeconomic status (SES).
[b]The Crovitz-Zener handedness questionnaire.[36]
[c]The Wechsler Adult Intelligence Scale (IQ) was estimated based on the Wechsler Test of Adult Reading for native English-speaking participants.[37]

of substance dependence (except nicotine), or having a first-degree relative with a psychotic disorder. SZ participants were excluded if they met criteria for substance dependence within the last year. Associations between medication dosage (chlorpromazine equivalents) and EEG-BOLD coupling are reported in the supplementary material. A trained research assistant, psychiatrist, or clinical psychologist conducted all diagnostic and clinical interviews, including the SCID-IV[39] and the Positive and Negative Syndrome Scale (PANSS).[40] The Sensory Gating Inventory (SGI)[41] was completed as a written questionnaire.

Study procedures were approved by the University of California at San Francisco and the San Francisco Veterans Affairs Medical Center Institutional Review Boards. All participants provided written informed consent.

EEG-fMRI Acquisition

Details of our acquisition and preprocessing protocols are described in the supplementary material and have been previously reported.[38,42] During acquisition, participants were instructed to keep their eyes open and fixate on a white cross displayed on a black screen for 6 min. Structural and fMRI data were collected using a 3T Siemens Skyra scanner using an echo planar imaging (EPI) sequence.

fMRI Preprocessing

Statistical Parametric Mapping 8 (SPM8; software) was used for image preprocessing, including motion correction and slice-time correction. We implemented aCompCor (anatomic component-based noise correction), a principal components-based approach for noise reduction.[43]

EEG Acquisition and Preprocessing

EEG data were collected from 32 scalp sites with an additional electrode placed on the lower back to monitor electrocardiogram (ECG). Data were recorded at 5 kHz and down-sampled to 250 Hz. MR gradient artifacts were removed using artifact subtraction and implemented in Brain Vision Analyzer 2.0.4.368 software (BrainProducts). The correction algorithm involved subtracting an artifact template from the raw data, using a baseline-corrected sliding average of 21 consecutive volumes to generate the template.[44]

Semi-automatic heartbeat detection was performed in Brain Vision Analyzer, where heartbeats were identified in the ECG channel that exhibited a high temporal correlation ($r > 0.5$) with a heartbeat template and within-range amplitude (0.6–1.7 mV). An average pulse curve is subtracted from the EEG separately for each heartbeat and channel.[45]

We implemented canonical correlation analysis as a blind source separation technique to remove electromyographic artifacts. This method is based on the observation that high-frequency noise in EEG (eg, muscle artifact) tends to show higher power at high frequencies than low frequencies, relative to EEG.[46,47] Artifactual repetition time (TR) intervals were identified from the Fully Automated Statistical Thresholding for EEG artifact Rejection (FASTER) toolbox (outliers >±3 SD from mean for multiple measures).[48] Independent components analysis was then performed on each participant in EEGLAB to remove rejected components. Noise components were identified by FASTER criteria as well as spatial correlations ($r > 0.8$) with eyeblink and ballistocardiac artifact templates. Examples of our artifact correction procedures are shown in the Supplementary Material.

Gamma and Aperiodic Parameter Estimation

Data from all 32 channels were segmented into 2-second epochs corresponding to whole brain acquisition time for each volume. We computed a Fourier transform within each epoch with a 2-second Hanning window (frequency resolution of 0.5 Hz) to obtain a power spectrum for each epoch. For each resulting power spectrum, we isolated periodic and aperiodic components using FOOOF (Fitting Oscillations and One Over F[9]) within the range of 1–50 Hz. We examined low gamma oscillations within a band range of 30–50 Hz that are consistent with definitions provided by the International Federation of Clinical Neurophysiology.[49] Mean power values for gamma and the aperiodic spectral exponent were extracted and entered into a parametric modulation analysis, discussed below. Group differences in gamma power, aperiodic power, and the Pearson correlation between gamma and aperiodic power (after Fisher's transformation) were determined from unpaired *t*-tests at electrode FC5 (selected based on the parametric modulation analysis below, results do not change for other electrodes).

Parametric Modulation Analysis

The details of our approach are reported in a prior manuscript.[38] Time series for gamma power and the aperiodic exponent were obtained for each 2-second TR and then *z*-scored. We utilized a whole-brain, parametric modulation analysis[50] using fluctuations in gamma and aperiodic EEG power dynamics as predictors for BOLD dynamics[51] in first-level fMRI analyses in SPM8. aCompCor noise components and motion parameters were included as nuisance regressors. For gamma and aperiodic EEG parameters, beta coefficients were estimated for each voxel's time series, resulting in beta images representing BOLD fluctuations predicted by EEG parameter variance. Beta images were normalized to the Montreal Neurological

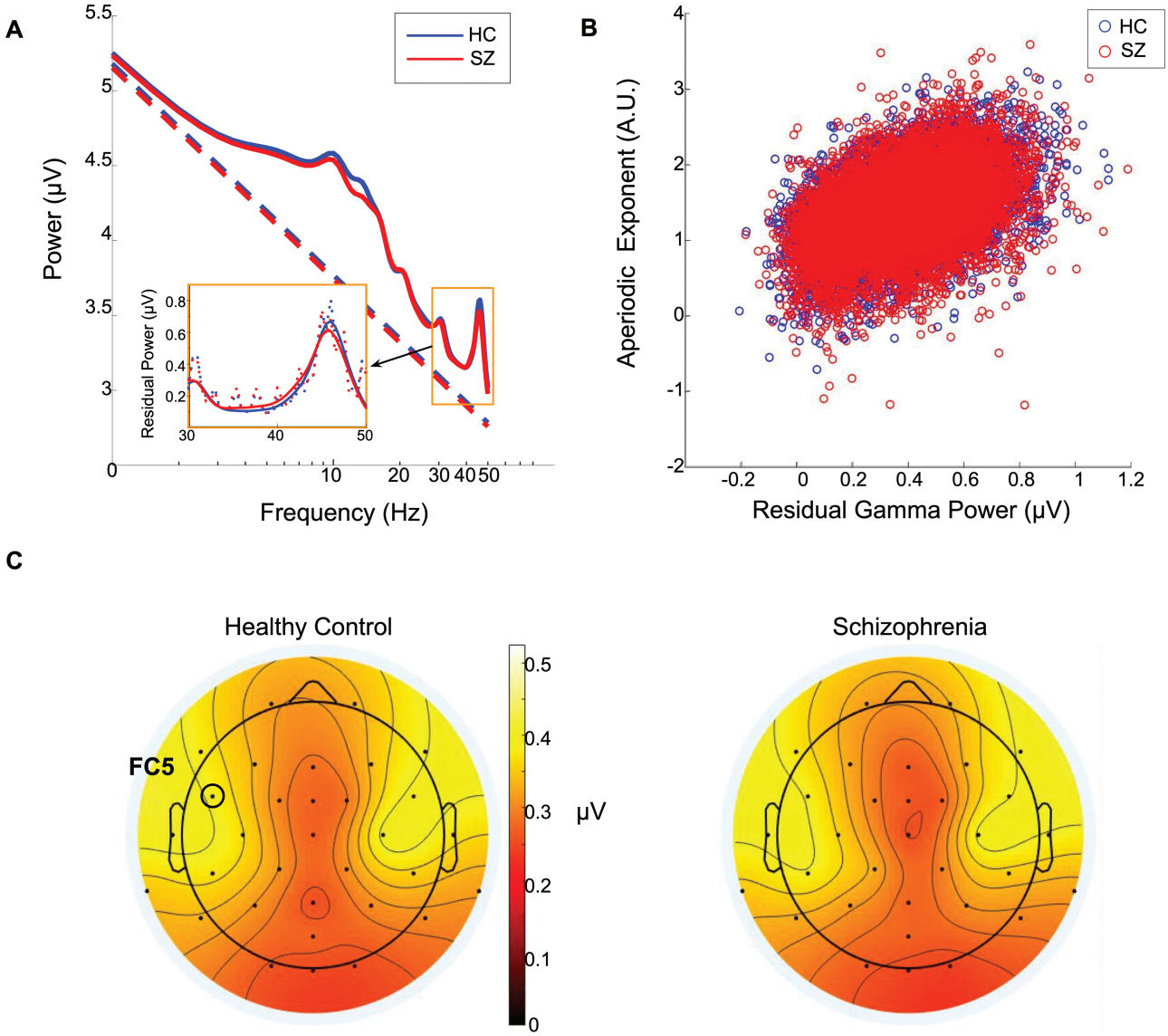

Fig. 1. (A) Grand average spectra, derived from the aperiodic (dashed line) and periodic fit (solid line) for all SZ (red) and HC participants (blue) from electrode FC5. Orange inset: Residual gamma power, which is measured after subtracting the aperiodic fit from the spectral data and calculating the average power in the 30–50 Hz range. (B) Scatter plot of residual gamma and the aperiodic exponent over all TR intervals at electrode FC5. (C) Scalp distribution of average residual gamma power in HC (left) and SZ (right) participants. Colorbar indicates the magnitude of power in microvolts. HC, healthy control; SZ, schizophrenia

Institute's (MNI) EPI template (http://www.bic.mni.mcgill.ca) and smoothed with a 6 mm Gaussian kernel.

We focused our analysis on group contrasts identified as EEG-fMRI clusters with significant differences in gamma and aperiodic BOLD coupling between SZ and HC. Main effects of gamma-BOLD coupling, run as separate models for each group, are shown in the supplementary material. The cluster-finding threshold was set to $P = .001$ (two-tailed) and a spatial extent of 10 voxels based on established criteria.[52,53] All cluster-level corrected P-values were also false discovery rate (FDR) corrected to account for multiple comparisons across channels. For significant clusters (pFDR < .05) beta coefficients were extracted and correlated with clinical measures to assess the relationship between EEG-BOLD coupling and symptoms. Significant clusters with group differences were identified from electrodes FC5 and T8.

Results

Gamma and Aperiodic Slope

There were no group differences in gamma power or aperiodic slope in EEG alone (gamma: $t(101) = 0.002$, $P = .99$; aperiodic slope: $t(101) = -0.87$, $P = .39$; figure 1A

Table 2. Clusters with a Significant Difference in EEG-BOLD Coupling between SZ and HC

EEG Parameter	Cluster	Voxels	Peak MNI (*x*, *y*, *z*)	pFDR
Residual Gamma power	Right STG	88	60, −13, 7	.038
	Left STG	73	−45, −19, 19	.052
Aperiodic slope	Left SFG/SMA	134	−9, 2, 70	.01

Note: EEG, electroencephalography; MNI, Montreal Neurologic Institute; STG, superior temporal gyri; SFG, superior frontal gyrus; SMA, supplementary motor area.

and 1C). For all participants, greater gamma power was associated with steeper slope (greater inhibition, mean $r = 0.52$; figure 1B) with no differences in slopes between HC and SZ participants ($t(101) = 0.1408$, $P = .89$).

EEG-BOLD Coupling

Whole-brain parametric modulation analyses revealed three clusters with an aberrant pattern of EEG-BOLD coupling in SZ (table 2). Gamma-BOLD coupling from 2 regions of the bilateral superior temporal gyri (STG, including the auditory cortex) was reduced in SZ (figure 2). In addition, BOLD activity in the left superior frontal gyrus (SFG, including the supplementary motor area [SMA]) showed an opposite direction of coupling in HC and SZ groups (figure 3). In the SFG cluster, HCs showed BOLD activity that was negatively coupled to the aperiodic exponent (flatter slope, more BOLD) whereas SZ showed BOLD activity that was positively coupled to the aperiodic exponent (steeper slope, more BOLD).

Scanner Sound Spectra

Given the presence of strong gamma-BOLD coupling in the auditory cortex with a gamma peak between 40 and 50 Hz (figure 1A), we examined whether gamma-BOLD coupling in this region might reflect auditory processing of scanner background sound. In a preliminary test of this hypothesis, we recorded low-fidelity scanner sound from the console during a "phantom" (EEG cap only, no human participant present) resting-state sequence and estimated the power spectral density of the audio signal. We observed distinct low frequency peaks in the audio signal between 30 and 100 Hz in the power spectrum reflecting complex repeating scanner pulse sounds at ~900 Hz (carrier frequency, figure 4B). A distinct peak was present in the range of our EEG analysis, particularly above 40 Hz in the gamma range (see figure 4C). This activity was not present in EEG data collected outside of the scanner nor in phantom EEG-fMRI recordings from the EEG cap (see Supplementary Material).

Symptoms and Sensory Gating

Within SZ, beta weights extracted from gamma-BOLD coupling in STG clusters inversely correlate with subjective self-report of sensory gating deficits as measured by the SGI (figure 5A and Supplementary Table S1). That is, deficient gamma-BOLD coupling in these regions was associated with worse sensory gating. Deficient gamma-BOLD in the R STG was also associated with overall symptom severity and positive symptom severity (figure 5B and Supplementary Table S1). The SGI was not correlated with total PANSS scores or any of the PANSS subscales (Supplementary Table S2). Including both symptom severity on the PANSS and SGI in the same model, did not change the significance of either as a predictor of gamma-BOLD coupling (both *P*s < .03).

Discussion

We investigated the hemodynamic correlates of ongoing E/I balance at rest by examining simultaneous BOLD coupling to fluctuations in gamma power and the aperiodic spectral slope in HC participants and participants with SZ. We found reduced BOLD coupling to gamma power in the STG in participants with SZ, including regions of the auditory cortex. Patients with worse subjective gating of sensory stimuli and more severe psychotic symptoms showed the most deficient BOLD coupling. SZ participants also showed inverse coupling to aperiodic slope in the SFG, specifically the supplementary motor cortex. We hypothesized that gamma oscillations in our paradigm might be entrained to the sounds generated by the MR scanner. In support of this hypothesis, we identified peaks in the gamma range from a spectral analysis of the audio signal generated during the resting state sequence that were not present during EEG recordings conducted outside of the scanner.

We suggest that the resting-state condition is not "at rest" but instead reflects sensory processing of scanner sound. Therefore, rs-fMRI paradigms may be an unavoidable but also semi-naturalistic paradigm to study background auditory sound processing in SZ, a population for whom sensory processing deficits are well-known and related to functional impairment.[1] Our findings have implications for the use of neuroimaging technology in psychiatric populations, such as SZ, that may be differentially impacted by environmental features, such as loud background sounds.

E/I Balance, Gamma, and Aperiodic Slope

A priori, we planned to examine gamma oscillations and aperiodic slope as putative indices reflecting E/I balance. For all participants, gamma power was correlated with aperiodic slope (increased power associated with a steeper slope), explaining about 25% of the variance in aperiodic slope. In contrast with our hypothesis, we

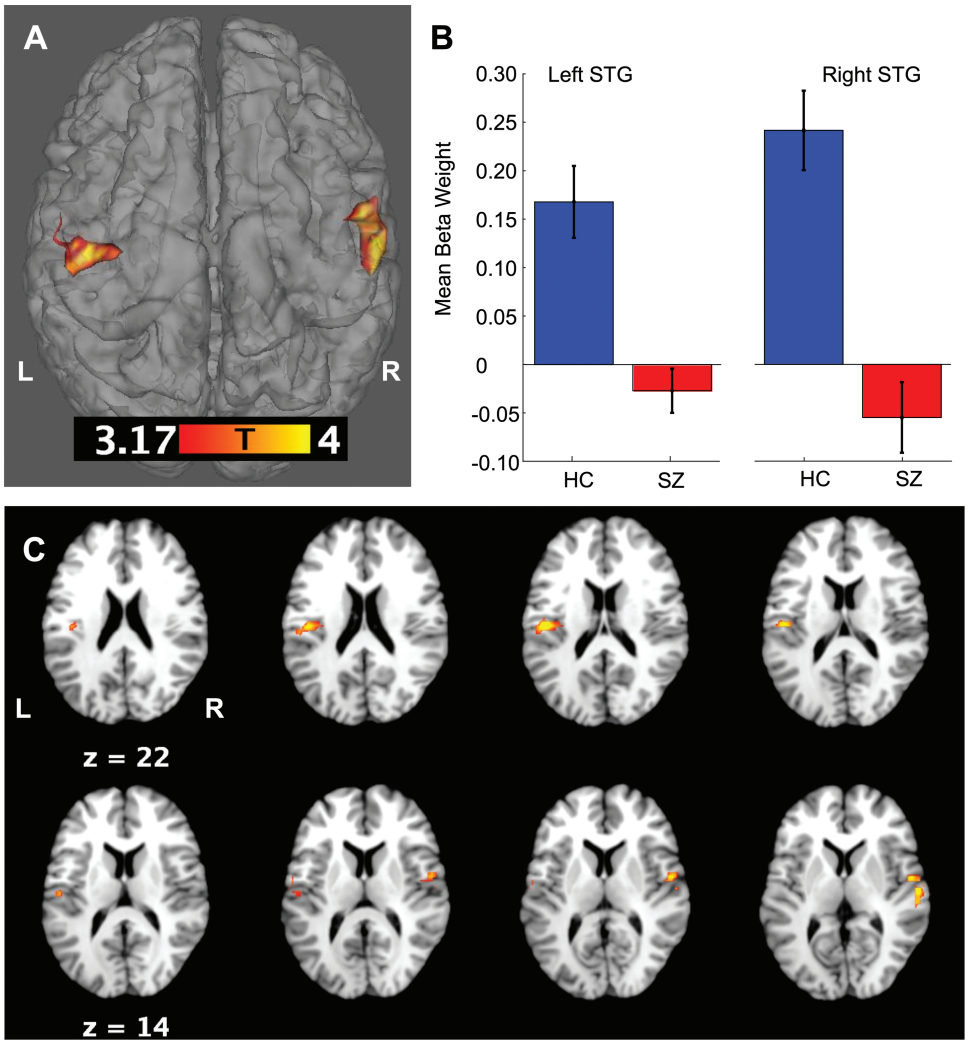

Fig. 2. (A) Two clusters identified deficient BOLD Coupling to Gamma power in SZ. The magnitude of the T-score (HC > SZ) is given by the colorbar. (B) Beta weights from the clusters shown in (A). (C) Axial sections that include the clusters shown in (A). HC, healthy control; SZ, schizophrenia.

observed no difference in either spectral slope or gamma power between HC and SZ. Atypical gamma oscillations are widely reported in SZ, with most studies reporting reduced power and phase locking of both evoked and resting-state oscillations.[54] However, results of resting-state studies are less consistent, with some studies also reporting *increased* gamma power during rest.[16,55] In contrast with gamma band studies, there is limited prior work examining the aperiodic slope in SZ with a preliminary report of reduced spectral exponent during a working memory task[56] and no apparent difference in another study.[57] Given that we are unable to identify group differences in either of our putative measures of E/I balance in the context of a simultaneous EEG-fMRI study, we suggest that features of the scanner environment, and scanner sound in particular (as we discuss below), are driving neural excitability and could be obscuring group differences.

Deficient Gamma-BOLD Coupling

HCs show coupling between gamma power and BOLD activity in the right and left STG, while participants with SZ show deficient gamma-BOLD coupling in these same regions. These regional findings align closely with our prior examination of EEG-BOLD coupling in SZ using joint independent component analysis in an auditory processing task.[42] In that study, we identified fMRI activation in the STG and middle temporal gyri associated with the N100 event-related potential (ERP), a component elicited 100 ms following an auditory stimulus. In the current study, we find similar activation in STG associated with gamma power. We, therefore, suggest that even in the absence of an explicit auditory task, scanner noise may induce STG gamma-BOLD coupling that reflects auditory processing.

Our investigation into the spectral features of the scanner environment revealed peaks near 40 Hz in the

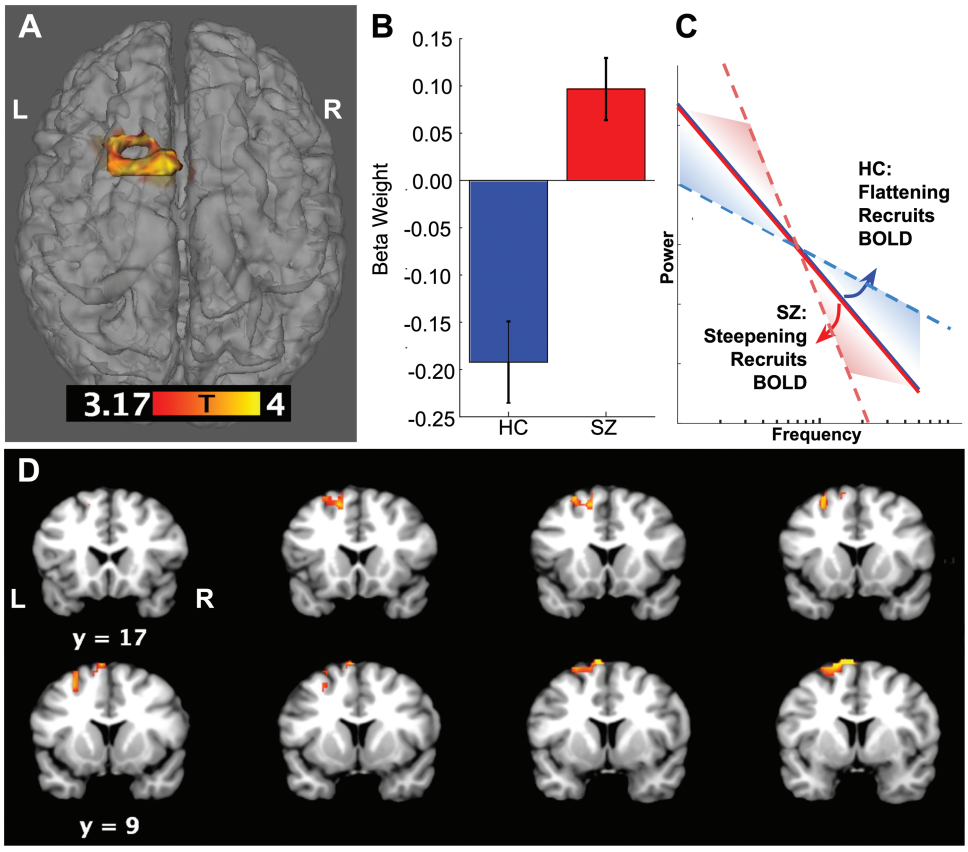

Fig. 3. (A) One cluster in the SFG identified an opposite pattern of aperiodic-BOLD coupling in HC and SZ participants. The magnitude of the T-score (SZ > HC) is given by the colorbar. (B) Beta weights derived from the cluster shown in (A) reveal positive coupling in SZ and negative coupling in HCs. (C) A graphical representation depicting the direction of aperiodic slope coupling to BOLD. SZ and HC participants show the same average spectral exponent (solid line). Fluctuation in the exponent is differentially coupled to BOLD in SZ vs HC (positive vs negative Beta weight from B): positive coupling yields a steeper slope (a greater spectral exponent, dashed red line) and negative coupling yields a flatter slope (smaller spectral exponent, dashed blue line). (D) Coronal sections that include the cluster shown in (A). HC, healthy control; SZ, schizophrenia; EEG, electroencephalography; SFG, superior frontal gyrus.

power spectrum that might reflect repeating scanner pulse sounds at ~900 Hz (carrier frequency). Furthermore, reduced STG gamma-BOLD coupling was associated with more severe sensory gating deficits; we speculate that gamma-BOLD coupling in the auditory cortex may reflect the neurophysiological processes involved with suppressing or gating irrelevant scanner sound. The association between gamma-BOLD activity and the SGI remained significant after controlling for PANSS total symptom severity. Nonetheless, differences in gamma-BOLD coupling could also reflect more general phenomena, such as differences in arousal or overall severity of psychopathology, as is suggested by the association between gamma-BOLD coupling and total symptoms.

Deficits in early auditory processing have been extensively reported in SZ,[1] with impaired gamma power[58] and auditory BOLD activation[59] reported during auditory paradigms. Most relevant to the current study are auditory steady-state response (ASSR) paradigms, in which participants with SZ show reduced power and phase-locking of gamma oscillations to rapidly repeating (40 Hz) auditory stimuli.[19–22,54] 40 Hz stimulus frequency is most effective for producing the superposition of transient neural responses (gamma entrainment)[60]; we speculate that the current results reflect gamma activity entrained to scanner sound pulses near 40 Hz.

Aperiodic-BOLD Coupling

HC and SZ participants showed opposite BOLD coupling relationships to the aperiodic slope in frontal regions. That is, a larger BOLD signal was associated with a flatter (more excitatory) slope in HCs and a steeper (more inhibitory) slope in SZ. This finding was localized to the SFG and regions of the SMA, which is also involved with auditory processing and particularly auditory imagery.[61,62] Notably, these findings overlap spatially with regions associated with auditory ERP components reported in our prior study.[42] We previously found BOLD activation in frontal regions including the SFG that was associated with the P200 ERP and is thought to index later auditory processing that is modulated by attention.

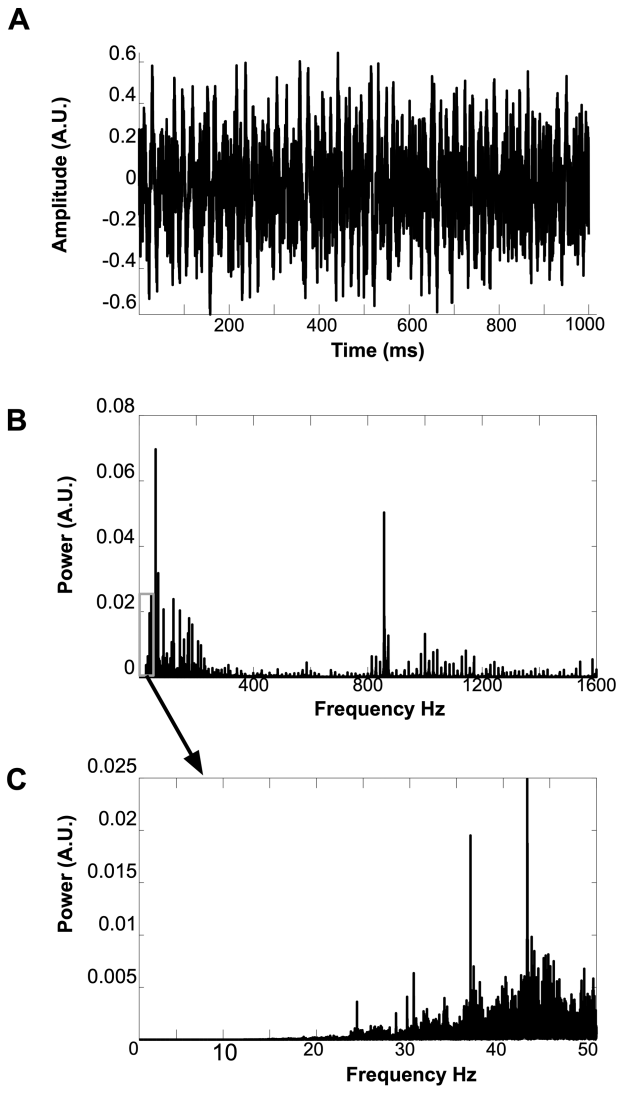

Fig. 4. (A) Tracing of the amplitude of the scanner sound signal recorded during the first second of the resting-state sequence. (B) Sound signal spectra of the 6-minute resting-state sequence. (C) Sound spectra within the range of EEG activity recorded in this experiment. EEG, electroencephalography.

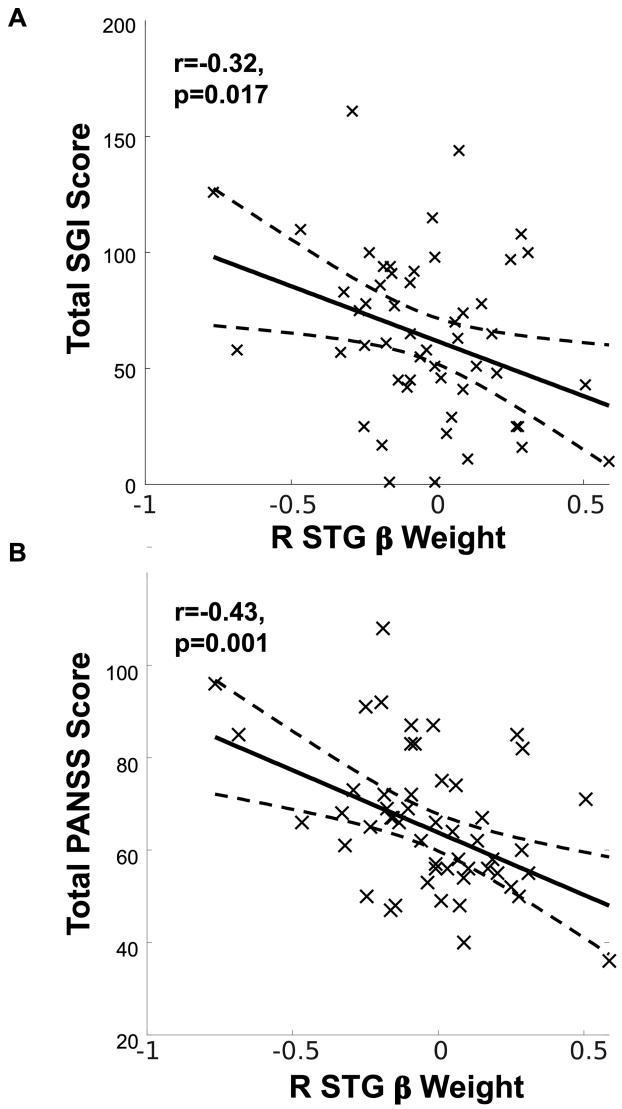

Fig. 5. (A) Total sensory gating inventory score (ordinate) inversely correlates with the strength of R STG Gamma-BOLD coupling SZ (abscissa). Regression line is given by the solid line, dashed lines indicate the 95% confidence interval. (B) Greater total symptoms on the PANSS (ordinate) inversely correlates with the strength of R-STG Gamma-BOLD coupling SZ (abscissa). SZ, schizophrenia; STG, superior temporal gyri; PANSS, Positive and Negative Syndrome Scale.

Our finding of altered aperiodic-BOLD coupling in the SFG may relate to attentional mechanisms involved in auditory processing of scanner sound. Participants with SZ show reduced frontal BOLD recruitment during task-relevant stimuli but allocate excessive resources to task-irrelevant stimuli.[63] Similar attentional mechanisms could influence the processing of MR scanner sound, and potentially as compensation for deficient sensory gating within primary auditory regions.

Broadly, these findings may be interpreted in the context of frontal inhibitory deficits in SZ and compensatory hemodynamic support. Our findings indicate that frontal metabolic work is required to maintain E/I balance functions in *opposite* directions in SZ and HC: increased metabolic work is required for excitation in HC and for inhibition in SZ. Thus, while we did not find evidence of altered aperiodic slope in SZ, we speculate that altered aperiodic-BOLD coupling may be indicative of compensatory metabolic resources required to maintain sufficient frontal inhibition in SZ.

Implications and Future Directions

In single modality, fMRI-only studies, ongoing resting-state neural signals are frequently attributed to internal processes and the default mode network (DMN).[64] Our focus on concurrent EEG-fMRI recordings reveals that

EEG activity may also be linked to stimulus-specific processing of the external environment. This processing might further interact with internal processing, or suggest individual differences in background processing, as we have observed within this population of SZ participants. Future studies might query participants about their experience in the scanner to derive post-hoc measures of attentional focus (eg, scanner sounds or self-referential thoughts). We hope that our work prompts a re-consideration of resting-state methodology in SZ. Future studies might examine if well-studied DMN connectivity differences might be impacted by participant attentional orientation while at rest.[32]

Limitations

Our study is primarily limited by the fact that we do not have unique and specific scanner sound parameters, including onset/offset timing, for direct correlation with EEG or BOLD signals on a scan-by-scan basis. While our results suggest that EEG-BOLD coupling plays a role in auditory processing, our paradigm was not specifically designed to test this hypothesis. EEG studies are needed that examine the scanner environment and sound, but in the absence of a magnetic field. Although we did not find group differences in resting-state aperiodic slope or gamma power, we cannot rule out the possibility that such differences would be present during a single modality EEG recording conducted outside of the scanner. For this reason, it is difficult to interpret our results in the context of other resting-state studies, particularly resting-state EEG studies that are recorded outside of a scanner. Additionally, EEG-fMRI artifacts such as head motion are not fully addressed in the absence of advanced approaches that adapt select EEG electrodes as motion sensors.[65] Therefore, it is possible that the gamma band activity we observed might be contaminated by movement or muscle artifacts exacerbated by the scanner environment. Future studies are needed to investigate how the scanner environment, including scanner sound, posture and being in an enclosed space might influence EEG activity.[66] These factors might differentially impact participants with SZ, indicating the need for detailed study of environmental scanner effects across clinical populations.

Supplementary Material

Supplementary material is available at https://academic.oup.com/schizophreniabulletin/.

Funding

This work was supported by grants from the National Institute of Mental Health (R01MH058262–17 to JMF) and the VA (Merit Review I01CX000497–06 and Senior Research Career Award to 1IK6CX002519 to JMF, IK1CX002089 to MSJ).

Conflict of Interest

Dr Jacob reported grants from the VA during the conduct of the study. Dr Mathalon reported grants from NIMH during the conduct of the study; consulting fees from Recognify Life Science, Syndesi Therapeutics, Cadent Therapeutics, and Gilgamesh Pharmaceuticals, outside the submitted work. Dr Ford reported grants from the VA and NIMH during the conduct of the study. No other disclosures were reported.

References

1. Javitt DC, Sweet RA. Auditory dysfunction in schizophrenia: integrating clinical and basic features. *Nat Rev Neurosci.* 2015;16:535–550.
2. Morrens M, Docx L, Walther S. Beyond boundaries: in search of an integrative view on motor symptoms in schizophrenia. *Front Psychiatry.* 2014;5:145.
3. Guo JY, Ragland JD, Carter CS. Memory and cognition in schizophrenia. *Mol Psychiatry.* 2019;24:633–642.
4. Yang, GJ, Murray, JD, Repovs, G, *et al*. Altered global brain signal in schizophrenia. *Proc Natl Acad Sci USA.* 2014;111:7438–7443.
5. Kaar SJ, Angelescu I, Marques TR, Howes OD. Pre-frontal parvalbumin interneurons in schizophrenia: a meta-analysis of post-mortem studies. *J Neural Transm.* 2019;126:1637–1651.
6. Blum BP, Mann JJ. The GABAergic system in schizophrenia. *Int J Neuropsychopharmacol.* 2002;5:159–179.
7. Sullivan CR, O'Donovan SM, McCullumsmith RE, Ramsey A. Defects in bioenergetic coupling in schizophrenia. *Biol Psychiatry.* 2018;83:739–750.
8. Sohal VS, Rubenstein JLR. Excitation-inhibition balance as a framework for investigating mechanisms in neuropsychiatric disorders. *Mol Psychiatry.* 2019;24:1248–1257.
9. Donoghue T, Haller M, Peterson EJ, *et al*. Parameterizing neural power spectra into periodic and aperiodic components. *Nat Neurosci.* 2020;23:1655–1665.
10. Atallah BV, Scanziani M. Instantaneous modulation of gamma oscillation frequency by balancing excitation with inhibition. *Neuron.* 2009;62:566–577.
11. Buzsáki G, Wang X-J. Mechanisms of gamma oscillations. *Annu Rev Neurosci.* 2012;35:203–225.
12. Lewis DA, Curley AA, Glausier JR, Volk DW. Cortical parvalbumin interneurons and cognitive dysfunction in schizophrenia. *Trends Neurosci.* 2012;35:57–67.
13. Sohal VS, Zhang F, Yizhar O, Deisseroth K. Parvalbumin neurons and gamma rhythms enhance cortical circuit performance. *Nature.* 2009;459:698–702.
14. Chung DW, Fish KN, Lewis DA. Pathological basis for deficient excitatory drive to cortical parvalbumin interneurons in schizophrenia. *Am J Psychiatry.* 2016;173:1131–1139.
15. Selten M, van Bokhoven H, Nadif Kasri N. Inhibitory control of the excitatory/inhibitory balance in psychiatric disorders. *F1000Res*. 2018;7:23.
16. Grent-'t-Jong T, Gross J, Goense J, *et al*. Resting-state gamma-band power alterations in schizophrenia reveal E/I-balance abnormalities across illness-stages. *eLife.* 2018;7:e37799.
17. Kwon JS, O'Donnell BF, Wallenstein GV, *et al*. Gamma frequency-range abnormalities to auditory stimulation in schizophrenia. *Arch Gen Psychiatry.* 1999;56:1001–1005.

18. Roach BJ, Mathalon DH. Event-related EEG time-frequency analysis: an overview of measures and an analysis of early gamma band phase locking in schizophrenia. *Schizophr Bull.* 2008;34:907–926.
19. Gandal MJ, Edgar JC, Klook K, Siegel SJ. Gamma synchrony: towards a translational biomarker for the treatment-resistant symptoms of schizophrenia. *Neuropharmacology.* 2012;62:1504–1518.
20. Thuné H, Recasens M, Uhlhaas PJ. The 40-Hz auditory steady-state response in patients with schizophrenia: a meta-analysis. *JAMA Psychiatry.* 2016;73:1145–1153.
21. Tada M, Kirihara K, Koshiyama D, *et al*. Gamma-band auditory steady-state response as a neurophysiological marker for excitation and inhibition balance: a review for understanding schizophrenia and other neuropsychiatric disorders. *Clin EEG Neurosci.* 2020;51:234–243.
22. Onitsuka T, Tsuchimoto R, Oribe N, *et al*. Neuronal imbalance of excitation and inhibition in schizophrenia: a scoping review of gamma-band ASSR findings. *Psychiatry Clin Neurosci.* 2022;76:610–619. doi:10.1111/pcn.13472.
23. Nguyen AT, Hetrick WP, O'Donnell BF, Brenner CA. Abnormal beta and gamma frequency neural oscillations mediate auditory sensory gating deficit in schizophrenia. *J Psychiatr Res.* 2020;124:13–21.
24. Kuga H, Onitsuka T, Hirano Y, *et al*. Increased BOLD signals elicited by high gamma auditory stimulation of the left auditory cortex in acute state schizophrenia. *EBioMedicine.* 2016;12:143–149.
25. Poil S-S, Hardstone R, Mansvelder HD, Linkenkaer-Hansen K. Critical-state dynamics of avalanches and oscillations jointly emerge from balanced excitation/inhibition in neuronal networks. *J Neurosci.* 2012;32:9817–9823.
26. Podvalny E, Noy N, Harel M, *et al*. A unifying principle underlying the extracellular field potential spectral responses in the human cortex. *J Neurophysiol.* 2015;114:505–519.
27. Gao R, Peterson EJ, Voytek B. Inferring synaptic excitation/inhibition balance from field potentials. *Neuroimage.* 2017;158:70–78.
28. Bridi MCD, Zong F-J, Min X, *et al*. Daily oscillation of the excitation-inhibition balance in visual cortical circuits. *Neuron.* 2020;105:621–629.e4.
29. Lendner JD, Helfrich RF, Mander BA, *et al*. An electrophysiological marker of arousal level in humans. *eLife.* 2020;9:e55092.
30. Colombo MA, Napolitani M, Boly M, *et al*. The spectral exponent of the resting EEG indexes the presence of consciousness during unresponsiveness induced by propofol, xenon, and ketamine. *Neuroimage.* 2019;189:631–644.
31. Ma Y, Shi W, Peng C-K, Yang AC. Nonlinear dynamical analysis of sleep electroencephalography using fractal and entropy approaches. *Sleep Med Rev.* 2018;37:85–93.
32. Benjamin C, Lieberman DA, Chang M, *et al*. The influence of rest period instructions on the default mode network. *Front Hum Neurosci.* 2010;4:218.
33. Kobald SO, Getzmann S, Beste C, *et al*. The impact of simulated MRI scanner background noise on visual attention processes as measured by the EEG. *Sci Rep.* 2016;6:28371.
34. Jacob MS, Roach BJ, Sargent KS, *et al*. Aperiodic measures of neural excitability are associated with anticorrelated hemodynamic networks at rest: A combined EEG-fMRI study. *Neuroimage.* 2021;5:1187.
35. Hollingshead, AB. *Four Factor Index of Social Status*. New Haven, CT: Yale University; 1975.
36. Crovitz HF, Zener K. A group-test for assessing hand- and eye-dominance. *Am J Psychol.* 1962;75:271–276.
37. Wechsler, D. *Wechsler Test of Adult Reading: WTAR*. San Antonio, TX: Psychological Corporation; 2001.
38. Jacob MS, Roach BJ, Sargent K, *et al*. Aperiodic measures of neural excitability are associated with anticorrelated hemodynamic networks at rest: a combined EEG-fMRI study. *Neuroimage.* 2021;245:118705.
39. First, MB, Spitzer, RL, Gibbon, M, *et al*. Structured clinical interview for DSM-IV axis I disorders, patient edition, January 1995 FINAL. In: *SCID-I/P Version 2.0.* New York, NY: Biometrics Research Department, New York State Psychiatric Institute; 1995.
40. Kay SR, Fiszbein A, Opler LA. The positive and negative syndrome scale (PANSS) for schizophrenia. *Schizophr Bull.* 1987;13:261–276.
41. Hetrick WP, Erickson MA, Smith DA. Phenomenological dimensions of sensory gating. *Schizophr Bull.* 2012;38:178–191.
42. Ford JM, Roach BJ, Palzes VA, Mathalon DH. Using concurrent EEG and fMRI to probe the state of the brain in schizophrenia. *Neuroimage Clin.* 2016;12:429–441.
43. Behzadi Y, Restom K, Liau J, Liu TT. A component based noise correction method (CompCor) for BOLD and perfusion based fMRI. *Neuroimage.* 2007;37:90–101.
44. Allen PJ, Josephs O, Turner R. A method for removing imaging artifact from continuous EEG recorded during functional MRI. *Neuroimage.* 2000;12:230–239.
45. Allen PJ, Polizzi G, Krakow K, Fish DR, Lemieux L. Identification of EEG events in the MR scanner: the problem of pulse artifact and a method for its subtraction. *Neuroimage.* 1998;8:229–239.
46. De Clercq W, Vergult A, Vanrumste B, *et al*. Canonical correlation analysis applied to remove muscle artifacts from the electroencephalogram. *IEEE Trans Biomed Eng.* 2006;53:2583–2587.
47. Riès S, Janssen N, Burle B, Alario F-X. Response-locked brain dynamics of word production. *PLoS One.* 2013;8:e58197.
48. Nolan H, Whelan R, Reilly RB. FASTER: fully automated statistical thresholding for EEG artifact rejection. *J Neurosci Methods.* 2010;192:152–162.
49. Babiloni C, Barry RJ, Başar E, *et al*. International federation of clinical neurophysiology (IFCN) - EEG research workgroup: recommendations on frequency and topographic analysis of resting state EEG rhythms. Part 1: applications in clinical research studies. *Clin Neurophysiol.* 2020;131:285–307.
50. Büchel C, Holmes AP, Rees G, Friston KJ. Characterizing stimulus–response functions using nonlinear regressors in parametric fMRI experiments. *Neuroimage.* 1998;8:140–148.
51. Laufs H, Krakow K, Sterzer P, *et al*. Electroencephalographic signatures of attentional and cognitive default modes in spontaneous brain activity fluctuations at rest. *Proc Natl Acad Sci USA.* 2003;100:11053–11058.
52. Woo C-W, Krishnan A, Wager TD. Cluster-extent based thresholding in fMRI analyses: pitfalls and recommendations. *Neuroimage.* 2014;91:412–419.
53. Eklund A, Nichols TE, Knutsson H. Cluster failure: Why fMRI inferences for spatial extent have inflated false-positive rates. *Proc Natl Acad Sci USA.* 2016;113:7900–7905.
54. Uhlhaas PJ, Singer W. Abnormal neural oscillations and synchrony in schizophrenia. *Nat Rev Neurosci.* 2010;11:100–113.
55. White RS, Siegel SJ. Cellular and circuit models of increased resting-state network gamma activity in schizophrenia. *Neuroscience.* 2016;321:66–76.

56. Peterson EJ, Rosen BQ, Campbell AM, *et al*. 1/f neural noise is a better predictor of schizophrenia than neural oscillations. *bioRxiv.* 2018;49:1134. doi:10.1101/113449.
57. Racz FS, Farkas K, Stylianou O, *et al*. Separating scale-free and oscillatory components of neural activity in schizophrenia. *Brain Behav*. 2021;11:e02047.
58. Spencer KM, Niznikiewicz MA, Shenton ME, McCarley RW. Sensory-evoked gamma oscillations in chronic schizophrenia. *Biol Psychiatry.* 2008;63:744–747.
59. Kiehl KA, Liddle PF. An event-related functional magnetic resonance imaging study of an auditory oddball task in schizophrenia. *Schizophr Res.* 2001;48:159–171.
60. Picton TW, Sasha John M, Dimitrijevic A, *et al*. Human auditory steady-state responses: Respuestas auditivas de estado estable en humanos. *Int J Audiol.* 2003;42:177–219.
61. McGuire PK, Silbersweig DA, Murray RM, David AS, Frackowiak RSJ, Frith CD. Functional anatomy of inner speech and auditory verbal imagery. *Psychol Med.* 1996;26:29–38.
62. Lima CF, Krishnan S, Scott SK. Roles of supplementary motor areas in auditory processing and auditory imagery. *Trends Neurosci.* 2016;39:527–542.
63. Hazlett EA, Buchsbaum MS, Zhang J, *et al*. Frontal-striatal-thalamic mediodorsal nucleus dysfunction in schizophrenia-spectrum patients during sensorimotor gating. *Neuroimage.* 2008;42:1164–1177.
64. Raichle ME. The brain's default mode network. *Annu Rev Neurosci.* 2015;38:433–447.
65. Jorge J, Grouiller F, Gruetter R, *et al*. Towards high-quality simultaneous EEG-fMRI at 7 T: Detection and reduction of EEG artifacts due to head motion. *Neuroimage* 2015;120:143–153.
66. Thibault RT, Lifshitz M, Jones JM, Raz A. Posture alters human resting-state. *Cortex.* 2014;58:199–205.